Path-integral formalism for stochastic resetting: Exactly solved examples and shortcuts to confinement

Édgar Roldán[1,*] and Shamik Gupta[2]

[1]*Max-Planck Institute for the Physics of Complex Systems, cfAED and GISC, Nöthnitzer Straße 38, 01187 Dresden, Germany*

[2]*Department of Physics, Ramakrishna Mission Vivekananda University, Belur Math, Howrah 711 202, West Bengal, India*

(Received 28 April 2017; revised manuscript received 16 July 2017; published 14 August 2017)

We study the dynamics of overdamped Brownian particles diffusing in conservative force fields and undergoing stochastic resetting to a given location at a generic space-dependent rate of resetting. We present a systematic approach involving path integrals and elements of renewal theory that allows us to derive analytical expressions for a variety of statistics of the dynamics such as (i) the propagator prior to first reset, (ii) the distribution of the first-reset time, and (iii) the spatial distribution of the particle at long times. We apply our approach to several representative and hitherto unexplored examples of resetting dynamics. A particularly interesting example for which we find analytical expressions for the statistics of resetting is that of a Brownian particle trapped in a harmonic potential with a rate of resetting that depends on the instantaneous energy of the particle. We find that using energy-dependent resetting processes is more effective in achieving spatial confinement of Brownian particles on a faster time scale than performing quenches of parameters of the harmonic potential.

DOI: 10.1103/PhysRevE.96.022130

I. INTRODUCTION

Changes are inevitable in nature, and those that are most dramatic, with often drastic consequences, are the ones that occur *all of a sudden*. A particular class of such changes comprises those in which the system during its temporal evolution makes a sudden jump (a "reset") to a fixed state or configuration. Many nonequilibrium processes are encountered across disciplines, e.g., in physics, biology, and information processing, which involve sudden transitions between different states or configurations. The erasure of a bit of information [1,2] by mesoscopic machines may be thought of as a physical process in which a memory device that is strongly affected by thermal fluctuations resets its state (0 or 1) to a prescribed erasure state [3–7]. In biology, resetting plays an important role *inter alia* in the sensing of extracellular ligands by single cells [8] and in the transcription of genetic information by macromolecular enzymes called RNA polymerases [9]. During RNA transcription, the recovery of RNA polymerases from inactive transcriptional pauses is the result of a kinetic competition between diffusion and resetting of the polymerase to an active state via RNA cleavage [9], as has been recently tested in high-resolution single-molecule experiments [10]. Also, there are ample examples of biochemical processes that initiate (i.e., reset) at random so-called *stopping* times [11–13], with the initiation in each instance occurring in different regions of space [14]. In addition, interactions play a key role in determining when and where a chemical reaction occurs [11], a fact that affects the statistics of the resetting process. For instance, in the above-mentioned example of recovery of RNA polymerase by the process of resetting, the interaction of the hybrid DNA-RNA may alter the time that a polymerase takes to recover from its inactive state [15]. It is therefore quite pertinent and timely to study resetting of mesoscopic systems that evolve under the influence of external or conservative force fields.

Simple diffusion subject to resetting to a given location at random times has emerged in recent years as a convenient theoretical framework in which to discuss the phenomenon of stochastic resetting [16–21]. The framework was later generalized to consider different choices of the resetting position [22,23], resetting of continuous-time random walks [24,25], Lévy [26] and exponential constant-speed flights [27], time-dependent resetting of a Brownian particle [28], and discussion of memory effects [29] and phase transitions in reset processes [30]. Stochastic resetting has also been invoked in the context of many-body dynamics, e.g., in reaction-diffusion models [31], fluctuating interfaces [32,33], interacting Brownian motion [34], and discussion of optimal search times in a crowded environment [35–38]. However, little is known about the statistics of stochastic resetting of Brownian particles that diffuse under the influence of force fields [39]—and that too in the presence of a rate of resetting that varies with space.

In this paper, we study the dynamics of overdamped Brownian particles immersed in a thermal environment, which diffuse under the influence of a force field and whose position may be stochastically reset to a given spatial location at a rate of resetting that has an essential dependence on space. We use an approach that allows us to obtain exact expressions for the transition probability prior to the first reset, the first reset-time distribution, and, most importantly, the stationary spatial distribution of the particle. The approach is based on a combination of the theory of renewals [40] and the Feynman-Kac path-integral formalism of treating stochastic processes [41–44] and consists in a mapping of the dynamics of the Brownian resetting problem to a suitable quantum mechanical evolution in imaginary time. We note that the Feynman-Kac formalism has been applied extensively in the past to discuss dynamical processes involving diffusion [45] and has, to the best of our knowledge, not been applied to discuss stochastic resetting. To demonstrate the utility of the approach, we consider several stochastic resetting problems (see Fig. 1): (i) free Brownian particles subject to a space-independent rate of resetting [Fig. 1(a)]; (ii) free Brownian particles subject to

*Corresponding author: edgar@pks.mpg.de

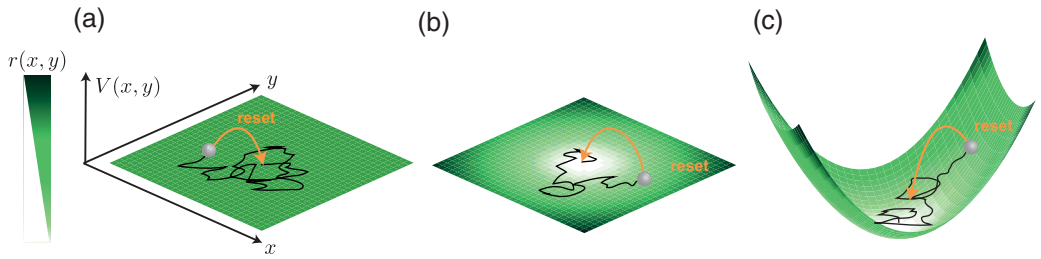

FIG. 1. Stochastic resetting of Brownian particles moving in force fields and subject to stochastic resetting at a rate that may depend on the space. Illustration of the motion of a single overdamped Brownian particle (gray sphere) that diffuses in two dimensions (x,y) in the presence of a conservative potential $V(x,y)$. The particle traces a stochastic trajectory (black curve) in the two-dimensional space until its position is reset at a random instant in time to its initial value (orange arrow); subsequent to the reset, the particle resumes its stochastic motion until the next reset happens. The rate of resetting $r(x,y)$ (left color bar) may depend on the position of the particle. We study three scenarios: (a) resetting of free Brownian particles under a space-independent rate of resetting; (b) resetting of free Brownian particles under a space-dependent rate of resetting; and (c) resetting of Brownian particles moving in force fields under a space-dependent rate of resetting.

resetting at a rate that depends quadratically on the distance to the origin [Fig. 1(b)]; and (iii) Brownian particles trapped in a harmonic potential and undergoing reset events at a rate that depends on the energy of the particle [Fig. 1(c)]. In this paper, we consider for purposes of illustration the corresponding scenarios in one dimension, although our general approach may be extended to higher dimensions. Remarkably, we obtain exact analytical expressions in all cases, notably, in cases ii and iii, where a standard treatment of the analytic solution using the Fokker-Planck approach may appear daunting, and whose relevance in physics may be explored in the context of, e.g., optically trapped colloidal particles and hopping processes in glasses and gels. We further explore the dynamical properties in case iii and compare the relaxation properties of dynamics corresponding to potential energy quenches and due to sudden activation of space-dependent stochastic resetting.

II. GENERAL FORMALISM

A. Model of study: Resetting of Brownian particles diffusing in force fields

Consider an overdamped Brownian particle diffusing in one dimension x in the presence of a time-independent force field $F(x) = -\partial_x V(x)$, with $V(x)$ denoting the potential energy landscape. The dynamics of the particle is described by a Langevin equation of the form

$$\frac{\mathrm{d}x}{\mathrm{d}t} = \mu F(x) + \eta(t), \tag{1}$$

where μ is the mobility of the particle, defined as the velocity per unit force. In Eq. (1), $\eta(t)$ is a Gaussian white noise, with the properties

$$\langle \eta(t) \rangle = 0, \quad \langle \eta(t)\eta(t') \rangle = 2D\delta(t-t'), \tag{2}$$

where $\langle \cdot \rangle$ denotes the average over noise realizations and $D>0$ is the diffusion coefficient of the particle, with the dimension of length squared over time. We assume that the Einstein relation holds: $D = k_B T \mu$, with T being the temperature of the environment and k_B being the Boltzmann constant. In addition to the dynamics, (1), the particle is subject to a stochastic resetting dynamics with a space-dependent resetting rate $r(x)$, whereby, while at position x at time t, the particle in the ensuing infinitesimal time interval $\mathrm{d}t$ either follows the dynamics, (1), with probability $1 - r(x)\mathrm{d}t$ or resets to a given reset destination $x^{(\mathrm{r})}$ with probability $r(x)\mathrm{d}t$. Our analysis holds for any arbitrary reset function $r(x)$, with the only obvious constraint $r(x) \geqslant 0 \; \forall \, x$; moreover, the formalism may be generalized to higher dimensions. In the following, we consider the reset location to be the same as the initial location x_0 of the particle, that is, $x^{(\mathrm{r})} = x_0$.

A quantity of obvious interest and relevance is the spatial distribution of the particle: What is the probability $P(x,t|x_0,0)$ that the particle is at position x at time t, given that its initial location is x_0? From the dynamics given in the preceding paragraph, it is straightforward to write the time evolution equation of $P(x,t|x_0,0)$,

$$\begin{aligned}\frac{\partial P(x,t|x_0,0)}{\partial t} &= -\mu \frac{\partial (F(x)P(x,t|x_0,0))}{\partial x} + D\frac{\partial^2 P(x,t|x_0,0)}{\partial x^2} \\ &\quad - r(x)P(x,t|x_0,0) + \int \mathrm{d}y r(y) P(y,t|x_0,0)\delta(x-x_0),\end{aligned} \tag{3}$$

where the first two terms on the right-hand side account for the contribution from the diffusion of the particle in the force field $F(x)$, while the last two terms stand for the contribution owing to the resetting of the particle: the third term represents the loss in probability arising from the resetting of the particle to x_0, while the fourth term denotes the gain in probability at location x_0 owing to resetting from all locations $x \neq x_0$. When it exists, the stationary distribution $P_{\mathrm{st}}(x|x_0)$ satisfies

$$\begin{aligned}0 &= -\mu \frac{\partial (F(x)P_{\mathrm{st}}(x|x_0))}{\partial x} + D\frac{\partial^2 P_{\mathrm{st}}(x|x_0)}{\partial x^2} \\ &\quad - r(x)P_{\mathrm{st}}(x|x_0) + \int \mathrm{d}y r(y) P_{\mathrm{st}}(y|x_0)\delta(x-x_0).\end{aligned} \tag{4}$$

It is evident that solving for either the time-dependent distribution $P(x,t|x_0,0)$ or the stationary distribution $P_{\mathrm{st}}(x|x_0)$ from Eq. (3) or (4), respectively, is a formidable task even with $F = 0$, unless the function $r(x)$ has simple forms. For example, in Ref. [17], the authors considered a solvable example with $F(x) = 0$, where the function $r(x)$ is 0 in a window around x_0 and is constant outside the window.

In this work, we employ a different approach to solve for the stationary spatial distribution, by invoking the path-integral formalism of quantum mechanics and by using elements of the theory of renewals. In this approach, we compute $P_{\rm st}(x|x_0)$, the stationary distribution *in the presence of reset events*, in terms of suitably defined functions that take into account the occurrence of trajectories that evolve *without undergoing any reset events* in a given time; see Eq. (30) below. This approach provides a viable alternative to obtaining the stationary spatial distribution by solving the Fokker-Planck equation, (4), which explicitly takes into account the occurrence of trajectories that evolve *while undergoing reset events* in a given time. As we demonstrate below, the method allows us to obtain exact expressions even in cases with nontrivial forms of $F(x)$ and $r(x)$.

B. Path-integral approach to stochastic resetting

Here, we invoke the well-established path-integral approach based on the Feynman-Kac formalism to discuss stochastic resetting. To proceed, let us first consider a representation of the dynamics in discrete times $t_i = i\Delta t$, with $i = 0,1,2,\ldots$ and $\Delta t > 0$ being a small time step. The dynamics in discrete times involves the particle at position x_i at time t_i either to reset and be at $x^{(\rm r)}$ at the next time step t_{i+1} with probability $r(x_i)\Delta t$ or to follow the dynamics given by Eq. (1) with probability $1 - r(x_i)\Delta t$. The position of the particle at time t_i is thus given by

$$x_i = \begin{cases} x_{i-1} + \Delta t(\mu \bar{F}(x_i) + \eta_i) & \text{with probability} \quad 1 - r(x_{i-1})\Delta t, \\ x^{(\rm r)} & \text{with probability} \quad r(x_{i-1})\Delta t, \end{cases} \tag{5}$$

where we have defined $\bar{F}(x_i) \equiv (F(x_{i-1}) + F(x_i))/2$ and have used the Stratonovich rule in discretizing the dynamics, (1), and where the time-discretized Gaussian white noise η_i satisfies

$$\langle \eta_i \eta_j \rangle = \sigma^2 \delta_{ij}, \tag{6}$$

with σ^2 a positive constant with the dimension of length squared over time squared. In particular, the joint probability distribution of the occurrence of a given realization $\{\eta_i\}_{1\leqslant i\leqslant N}$ of the noise, with N being a positive integer, is given by

$$P[\{\eta_i\}] = \left(\frac{1}{2\pi\sigma^2}\right)^{N/2} \exp\left(-\frac{1}{2\sigma^2}\sum_{i=1}^{N}\eta_i^2\right). \tag{7}$$

In the absence of any resetting and forces, the displacement of the particle at time $t \equiv N\Delta t$ from the initial location is given by $\Delta x \equiv x_N - x_0 = \Delta t \sum_{i=1}^{N} \eta_i$, so that the mean-squared displacement is $\langle (\Delta x)^2 \rangle = \sigma^2 N (\Delta t)^2$. In the continuous-time limit, $N \to \infty$, $\Delta t \to 0$, keeping the product $N\Delta t$ fixed and finite and equal to t, the mean-squared displacement becomes $\langle (\Delta x)^2 \rangle = 2Dt$, with $D \equiv \lim_{\sigma\to\infty, \Delta t\to 0} \sigma^2 \Delta t/2$.

1. The propagator prior to first reset

What is the probability of occurrence of particle trajectories that start at position x_0 and end at a given location x at time $t = N\Delta t$ without undergoing any reset event? From the discrete-time dynamics given by Eq. (5) and the joint distribution, (7), the probability of occurrence of a given particle trajectory $\{x_i\}_{0\leqslant i\leqslant N} \equiv \{x_0, x_1, x_2, \ldots, x_{N-1}, x_N = x\}$ is given by

$$\begin{aligned} &P_{\rm no\ res}[\{x_i\}] \\ &= \det(\mathcal{J}) \left(\frac{1}{2\pi\sigma^2}\right)^{N/2} \\ &\quad \times \prod_{i=1}^{N} \exp\left(-\frac{(x_i - x_{i-1} - \mu\bar{F}(x_i)\Delta t)^2}{2\sigma^2(\Delta t)^2}\right) \\ &\quad \times \prod_{i=0}^{N-1} (1 - r(x_i)\Delta t). \end{aligned} \tag{8}$$

Here, the factor $\prod_{i=0}^{N-1}(1 - r(x_i)\Delta t)$ enforces the condition that the particle has not reset at any of the instants t_i, $i = 0,1,2,\ldots,N-1$, while $\mathcal{J}$ is the Jacobian matrix for the transformation $\{\eta_i\} \to \{x_i\}$, which is obtained from Eq. (5) as $\mathcal{J}_{1\leqslant i,j\leqslant N} \equiv (\frac{\partial \eta_i}{\partial x_j})$ or, equivalently,

$$\mathcal{J} = \begin{pmatrix} \frac{1}{\Delta t} - \frac{\mu F'(x_1)}{2} & 0 & 0 & \ldots \\ -\frac{1}{\Delta t} - \frac{\mu F'(x_1)}{2} & \frac{1}{\Delta t} - \frac{\mu F'(x_2)}{2} & 0 & \ldots \\ \vdots & \vdots & \vdots & \vdots \end{pmatrix}_{N\times N}, \tag{9}$$

with primes denoting derivative with respect to x. One thus has

$$\begin{aligned} \det(\mathcal{J}) &= \left(\frac{1}{\Delta t}\right)^N \prod_{i=1}^{N}\left(1 - \frac{\Delta t \mu F'(x_i)}{2}\right) \\ &\simeq \left(\frac{1}{\Delta t}\right)^N \exp\left(-\sum_{i=1}^{N}\frac{\Delta t \mu F'(x_i)}{2}\right), \end{aligned} \tag{10}$$

where, in obtaining the last step, we have used the smallness of Δt. Thus, for small Δt, we get

$$\begin{aligned} &P_{\rm no\ res}[\{x_i\}] \\ &= \left(\frac{1}{2\pi\sigma^2(\Delta t)^2}\right)^{N/2} \\ &\quad \times \prod_{i=1}^{N} \exp\left(-\frac{(x_i - x_{i-1} - \mu\bar{F}(x_i)\Delta t)^2}{2\sigma^2(\Delta t)^2} - \frac{\Delta t \mu F'(x_i)}{2}\right) \\ &\quad \times \prod_{i=0}^{N-1} \exp\left(-r(x_i)\Delta t\right) \\ &= \left(\frac{1}{2\pi\sigma^2(\Delta t)^2}\right)^{N/2} \exp(\Delta t[r(x_N) - r(x_0)]) \\ &\quad \times \exp\left(-\Delta t \sum_{i=1}^{N}\left[\frac{[(x_i - x_{i-1} - \mu\bar{F}(x_i)\Delta t)/\Delta t]^2}{2\sigma^2 \Delta t} \right.\right. \\ &\quad \left.\left. + \frac{\mu F'(x_i)}{2} + r(x_i)\right]\right). \end{aligned} \tag{11}$$

From Eq. (11), it follows by considering all possible trajectories that the probability density that the particle, while starting at position x_0, will end at a given location x at time $t = N\Delta t$ without having undergone any reset event is given by

$$\begin{aligned} &P_{\text{no res}}(x,t|x_0,0) \\ &= \left(\frac{1}{2\pi\sigma^2(\Delta t)^2}\right)^{N/2} \exp(\Delta t[r(x)-r(x_0)]) \\ &\times \prod_{i=1}^{N-1}\int_{-\infty}^{\infty} \mathrm{d}x_i \\ &\times \exp\left(-\Delta t\sum_{i=1}^{N}\left[\frac{[(x_i - x_{i-1} - \mu\bar{F}(x_i)\Delta t)/\Delta t]^2}{2\sigma^2\Delta t}\right.\right. \\ &\left.\left. + \frac{\mu F'(x_i)}{2} + r(x_i)\right]\right). \end{aligned} \tag{12}$$

In the limit of continuous time, defining $\mathcal{D}x(t) \equiv \lim_{N\to\infty}\left(\frac{1}{4\pi D\Delta t}\right)^{N/2}\prod_{i=1}^{N-1}\int_{-\infty}^{\infty}\mathrm{d}x_i$, one gets the exact expression for the corresponding probability density as the path integral

$$P_{\text{no res}}(x,t|x_0,0) = \int_{x(0)=x_0}^{x(t)=x}\mathcal{D}x(t)\exp\left(-S_{\text{res}}[\{x(t)\}]\right), \tag{13}$$

where, on the right-hand side of Eq. (13), we have introduced the *resetting action* as

$$S_{\text{res}}[\{x(t)\}] = \int_0^t \mathrm{d}t\left[\frac{[(\mathrm{d}x/\mathrm{d}t) - \mu F(x)]^2}{4D} + \frac{\mu F'(x)}{2} + r(x)\right]. \tag{14}$$

Invoking the Feynman-Kac formalism, we identify the path integral on the right-hand side of Eq. (13) with the propagator of a quantum mechanical evolution in (negative) imaginary time due to a quantum Hamiltonian H_q, to get

$$P_{\text{no res}}(x,t|x_0,0) = \exp\left(\frac{\mu}{2D}\int_{x_0}^{x} F(x)\mathrm{d}x\right) G_q(x,-it|x_0,0), \tag{15}$$

with

$$G_q(x,-it|x_0,0) \equiv \langle x|\exp(-H_q t)|x_0\rangle, \tag{16}$$

where the quantum Hamiltonian is

$$H_q \equiv -\frac{1}{2m_q}\frac{\partial^2}{\partial x^2} + V_q(x), \tag{17}$$

the mass in the equivalent quantum problem is

$$m_q \equiv \frac{1}{2D}, \tag{18}$$

and the quantum potential is given by

$$V_q(x) \equiv \frac{\mu^2(F(x))^2}{4D} + \frac{\mu F'(x)}{2} + r(x). \tag{19}$$

Note that in the quantum propagator in Eq. (16), Planck's constant has been set to unity, $\hbar = 1$, while the time τ of propagation is imaginary: $\tau = -it$ [46]. Since the Hamiltonian contains no explicit time dependence, the propagator $G_q(x,-it|x_0,0)$ is effectively a function of the time t it takes to propagate from the initial location x_0 to the final location x, and not individually of the initial and final times. Let us note that, using $D = k_B T\mu$, the prefactor equals $\exp(-Q(t)/2k_BT)$, where $Q(t) \equiv \int_{x_0}^{x}\partial_x V(x)\,\mathrm{d}x$ is the heat absorbed by the particle from the environment along the trajectory $\{x(t)\}$ [47,48].

2. Distribution of the first-reset time

Let us now determine the probability of occurrence of trajectories that start at position x_0 and reset for the first time at time t. In terms of $P_{\text{no res}}(x,t|x_0,0)$, one gets this probability density as

$$P_{\text{res}}(t|x_0) = \int_{-\infty}^{\infty}\mathrm{d}y r(y) P_{\text{no res}}(y,t|x_0,0), \tag{20}$$

since, by the very definition of $P_{\text{res}}(t|x_0)$, a reset has to happen only at the final time t when the particle has reached the location y, where y may in principle take any value in the interval $[-\infty,\infty]$. The probability density $P_{\text{res}}(t|x_0)$ is normalized as $\int_0^\infty \mathrm{d}t\, P_{\text{res}}(t|x_0) = 1$.

3. Spatial time-dependent probability distribution

Using renewal theory, we now show that knowing $P_{\text{no res}}(x,t|x_0,0)$ and $P_{\text{res}}(t|x_0)$ is sufficient to obtain the spatial distribution of the particle at any time t. The probability density that the particle is at x at time t when starting from x_0 is given by

$$\begin{aligned} &P(x,t|x_0,0) \\ &= P_{\text{no res}}(x,t|x_0,0) \\ &\quad + \int_0^t \mathrm{d}\tau\int_{-\infty}^{\infty}\mathrm{d}y r(y) P(y,t-\tau|x_0,0) P_{\text{no res}}(x,t|x_0,t-\tau) \\ &= P_{\text{no res}}(x,t|x_0,0) \\ &\quad + \int_0^t \mathrm{d}\tau\, R(t-\tau|x_0) P_{\text{no res}}(x,t|x_0,t-\tau), \end{aligned} \tag{21}$$

where we have defined the probability density of resetting at time t as

$$R(t|x_0) \equiv \int_{-\infty}^{\infty}\mathrm{d}y r(y) P(y,t|x_0,0). \tag{22}$$

One may easily understand Eq. (21) by invoking the theory of renewals [40] and realizing that the dynamics is renewed each time the particle resets to x_0. This may be seen as follows. The particle starting from x_0 may reach x at time t by experiencing not a single reset; the corresponding contribution to the spatial distribution is given by the first term on the right-hand side of Eq. (21). The particle may also reach x at time t by experiencing the last reset event (i.e., the last renewal) at time $t-\tau$, with $\tau \in [0,t]$, and then propagating from the reset location $x^{(\mathrm{r})} = x_0$ to x without experiencing any further reset, where the last reset may take place at rate $r(y)$ from any location $y \in [-\infty,\infty]$ where the particle happened to be at time $t-\tau$; such contributions are represented by the second term on the right-hand side of Eq. (21). The spatial distribution is normalized as $\int_{-\infty}^{\infty}\mathrm{d}x\, P(x,t|x_0,0) = 1$ for all possible values of x_0 and t.

Multiplying both sides of Eq. (21) by $r(x)$ and then integrating over x, we get

$$R(t|x_0) = \int_{-\infty}^{\infty} dx r(x) P_{\text{no res}}(x,t|x_0,0) + \int_0^t d\tau \left[\int_{-\infty}^{\infty} dx r(x) P_{\text{no res}}(x,t|x_0,t-\tau) \right] \times R(t-\tau|x_0). \quad (23)$$

The bracketed quantity on the right-hand side of (23) is nothing but $P_{\text{res}}(\tau|x_0)$, so we get

$$R(t|x_0) = P_{\text{res}}(t|x_0) + \int_0^t d\tau\, P_{\text{res}}(\tau|x_0) R(t-\tau|x_0). \quad (24)$$

Taking the Laplace transform on both sides of Eq. (24), we get

$$\widetilde{R}(s|x_0) = \widetilde{P}_{\text{res}}(s|x_0) + \widetilde{P}_{\text{res}}(s|x_0)\widetilde{R}(s|x_0), \quad (25)$$

where $\widetilde{R}(s|x_0)$ and $\widetilde{P}_{\text{res}}(s|x_0)$ are, respectively, the Laplace transforms of $R(t|x_0)$ and $P_{\text{res}}(t|x_0)$. Solving for $\widetilde{R}(s|x_0)$ from Eq. (25) yields

$$\widetilde{R}(s|x_0) = \frac{\widetilde{P}_{\text{res}}(s|x_0)}{1 - \widetilde{P}_{\text{res}}(s|x_0)}. \quad (26)$$

Next, taking the Laplace transform with respect to time on both sides of Eq. (21), we obtain

$$\widetilde{P}(x,s|x_0,0) = (1 + \widetilde{R}(s|x_0))\widetilde{P}_{\text{no res}}(x,s|x_0) = \frac{\widetilde{P}_{\text{no res}}(x,s|x_0)}{1 - \widetilde{P}_{\text{res}}(s|x_0)}, \quad (27)$$

where we have used Eq. (26) to obtain the last equality. An inverse Laplace transform of Eq. (27) yields the time-dependent spatial distribution $P(x,t|x_0,0)$.

4. Stationary spatial distribution

Upon applying the final value theorem, one may obtain the stationary spatial distribution as

$$P_{\text{st}}(x|x_0) = \lim_{s\to 0} s\,\widetilde{P}(x,s|x_0,0) = \lim_{s\to 0} s \frac{\widetilde{P}_{\text{no res}}(x,s|x_0)}{1 - \widetilde{P}_{\text{res}}(s|x_0)}, \quad (28)$$

provided the stationary distribution [i.e., $\lim_{t\to\infty} P(x,t|x_0,0)$] exists. Now, since $P_{\text{res}}(t|x_0)$ is normalized to unity, $\int_0^\infty dt\, P_{\text{res}}(t|x_0) = 1$, we may expand its Laplace transform to leading orders in s as $\widetilde{P}_{\text{res}}(s|x_0) \equiv \int_0^\infty dt \exp(-st) P_{\text{res}}(t|x_0) = 1 - s\langle t\rangle_{\text{res}} + O(s^2)$, provided that the mean first-reset time $\langle t\rangle_{\text{res}}$, defined as

$$\langle t\rangle_{\text{res}} \equiv \int_0^\infty dt\, t\, P_{\text{res}}(t|x_0), \quad (29)$$

is finite. Similarly, we may expand $\widetilde{P}_{\text{no res}}(x,s|x_0,0)$ to leading orders in s as $\widetilde{P}_{\text{no res}}(x,s|x_0,0) = \int_0^\infty dt\, P_{\text{no res}}(x,t|x_0,0) - s\int_0^\infty dt\, t\, P_{\text{no res}}(x,t|x_0,0) + O(s^2)$, provided that $\int_0^\infty dt\, t\, P_{\text{no res}}(x,t|x_0,0)$ is finite. From Eq. (28), we thus find the stationary spatial distribution to be given by the integral over all times of the propagator prior to first reset divided by the mean first-reset time:

$$P_{\text{st}}(x|x_0) = \frac{1}{\langle t\rangle_{\text{res}}} \int_0^\infty dt\, P_{\text{no res}}(x,t|x_0,0). \quad (30)$$

III. EXACTLY SOLVED EXAMPLES

A. Free particle with space-independent resetting

Let us first consider the simplest case of free diffusion at a space-independent rate of resetting $r(x) = r$, with r a positive constant having the dimension of inverse time. Here, upon using Eq. (15) with $F(x) = 0$, we have

$$P_{\text{no res}}(x,t|x_0,0) = G_q(x,-it|x_0,0) = \langle x|\exp(-H_q t)|x_0\rangle, \quad (31)$$

where the quantum Hamiltonian is in this case, following Eqs. (17)–(19), given by

$$H_q = -\frac{1}{2m_q}\frac{\partial^2}{\partial x^2} + r, \quad m_q = \frac{1}{2D}, \quad \hbar = 1. \quad (32)$$

Since in the present situation, the effective quantum potential $V_q(x) = r$ is space independent, we may rewrite Eq. (31) as

$$P_{\text{no res}}(x,t|x_0,0) = \exp(-rt) G_q(x,-it|x_0,0), \quad (33)$$

with

$$G_q(x,-it|x_0,0) \equiv \langle x|\exp(-H_q t)|x_0\rangle, \quad (34)$$

where the quantum Hamiltonian is now that of a free particle:

$$H_q \equiv -\frac{1}{2m_q}\frac{\partial^2}{\partial x^2}, \quad m_q = \frac{1}{2D}, \quad \hbar = 1. \quad (35)$$

Therefore, the statistics of resetting of a free particle under a space-independent rate of resetting may be found from the quantum propagator of a free particle, which is given by [42]

$$G_q(x,\tau|x_0,0) = \sqrt{\frac{m_{\text{q}}}{2\pi\hbar i\tau}} \exp\left(-\frac{m_q(x-x_0)^2}{2\hbar i\tau}\right). \quad (36)$$

Plugging into Eq. (36) the parameters in Eq. (35) together with $\tau = -it$, we have

$$G_q(x,-it|x_0,0) = \frac{1}{\sqrt{4\pi Dt}} \exp\left(-\frac{(x-x_0)^2}{4Dt}\right). \quad (37)$$

Using Eq. (37) in Eq. (33), we thus obtain

$$P_{\text{no res}}(x,t|x_0,0) = \frac{\exp(-rt)}{\sqrt{4\pi Dt}} \exp\left(-\frac{(x-x_0)^2}{4Dt}\right), \quad (38)$$

and hence, the distribution of the first-reset time may be found upon using Eq. (20),

$$P_{\text{res}}(t|x_0) = r\exp(-rt)\frac{1}{\sqrt{4\pi Dt}} \int_{-\infty}^{\infty} dx \exp\left(-\frac{(x-x_0)^2}{4Dt}\right) = r\exp(-rt), \quad (39)$$

which is normalized to unity, $\int_0^\infty dt\, P_{\text{res}}(t|x_0) = 1$, as expected.

Using Eq. (39), we get $\widetilde{P}_{\text{res}}(s|x_0) = r/(s+r)$, so that Eq. (26) yields $\widetilde{R}(s|x_0) = r/s$. An inverse Laplace transform yields $R(t|x_0) = r$, as also follows from Eq. (22) by substituting $r(y) = r$ and noting that $P(y,t|x_0,0)$ is normalized with respect to y.

Next, the probability density that the particle is at x at time t, when starting from x_0, is obtained upon using Eq. (21) as

$$P(x,t|x_0,0) = \frac{\exp(-rt)}{\sqrt{4\pi D\tau}} \exp\left(-(x-x_0)^2/(4Dt)\right) + r\int_0^t \mathrm{d}\tau \frac{\exp(-r\tau)}{\sqrt{4\pi D\tau}} \exp\left(-(x-x_0)^2/(4D\tau)\right). \tag{40}$$

Taking the limit $t \to \infty$, we obtain the stationary spatial distribution as

$$P_{\mathrm{st}}(x|x_0) = r\int_0^\infty \mathrm{d}\tau \exp(-r\tau) \frac{\exp\left(-(x-y)^2/(4D\tau)\right)}{\sqrt{4\pi D\tau}}, \tag{41}$$

which may also be obtained by using Eqs. (30) and (38) and, also, Eq. (39), which implies that $\langle t\rangle_{\mathrm{res}} = 1/r$. From Eq. (40), we obtain an exact expression for the time-dependent spatial distribution as

$$P(x,t|x_0,0) = \frac{\exp(-rt)\exp\left(-(x-x_0)^2/4Dt\right)}{\sqrt{4\pi Dt}} + \frac{\exp\left(-\frac{|x-x_0|}{\sqrt{D/r}}\right)\mathrm{erfc}\left(\frac{|x-x_0|}{\sqrt{4Dt}} - \sqrt{rt}\right)}{\sqrt{4D/r}} - \frac{\exp\left(\frac{|x-x_0|}{\sqrt{D/r}}\right)\mathrm{erfc}\left(\frac{|x-x_0|}{\sqrt{4Dt}} + \sqrt{rt}\right)}{\sqrt{4Dt}}, \tag{42}$$

while Eq. (41) yields the exact stationary distribution as

$$P_{\mathrm{st}}(x|x_0) = \frac{1}{2\sqrt{D/r}} \exp\left(-\frac{|x-x_0|}{\sqrt{D/r}}\right), \tag{43}$$

where $\mathrm{erfc}(x) \equiv (2/\sqrt{\pi})\int_x^\infty \mathrm{d}t \exp(-t^2)$ is the complementary error function. The stationary distribution, (43), may be put in the scaling form

$$P_{\mathrm{st}}(x|x_0) = \frac{1}{2\sqrt{D/r}} \mathcal{R}\left(\frac{|x-x_0|}{\sqrt{D/r}}\right), \tag{44}$$

where the scaling function is given by $\mathcal{R}(y) \equiv \exp(-y)$. For the particular case $x_0 = 0$, Eq. (43) matches the result derived in Ref. [16]. Note that the steady-state distribution, (44), exhibits a cusp at the resetting location x_0. Since the resetting location is taken to be the same as the initial location, over time the particle visits the initial location repeatedly, thereby keeping a memory of the latter that makes an explicit appearance even in the long-time stationary state.

B. Free particle with "parabolic" resetting

We now study the dynamics of a free Brownian particle whose position is reset to the initial position x_0 at a rate of resetting that is proportional to the square of the current position of the particle. In this case, we have $r(x) = \alpha x^2$, with $\alpha > 0$ having the dimension of $1/((\mathrm{Length})^2\mathrm{Time})$. From Eqs. (15) and (16), and given that in this case $F(x) = 0$, we get

$$P_{\text{no res}}(x,t|x_0,0) = G_q(x,-it|x_0,0) = \langle x|\exp(-H_q t)|x_0\rangle, \tag{45}$$

with the Hamiltonian obtained from Eq. (17) by setting $V_q(x) = \alpha x^2$:

$$H_q = -\frac{1}{2m_q}\frac{\partial^2}{\partial x^2} + \alpha x^2, \quad m_q = \frac{1}{2D}, \quad \hbar = 1. \tag{46}$$

We thus see that the statistics of resetting of a free particle subject to a "parabolic" rate of resetting may be found from the propagator of a quantum harmonic oscillator. Following Schulman [42], a quantum harmonic oscillator with the Hamiltonian given by

$$H_q = -\frac{1}{2m_{\mathrm{q}}}\frac{\partial^2}{\partial x^2} + \frac{1}{2}m_q\omega_q^2 x^2, \tag{47}$$

with m_q and ω_q being the mass and the frequency of the oscillator, has the quantum propagator

$$G_q(x,\tau|x_0,0) = \sqrt{\frac{m_q\omega_{\mathrm{q}}}{2i\pi\hbar\sin\omega_q\tau}} \times \exp\left(\frac{i\omega_q}{2\hbar\sin\omega_q\tau}\left[\left(x^2+x_0^2\right)\cos\omega_q\tau - 2xx_0\right]\right). \tag{48}$$

Using the parameters given in Eq. (46) and substituting $\tau = -it$ and $\omega_q = \sqrt{4D\alpha}$ in Eq. (48), we have

$$G_q(x,-it|x_0,0) = \frac{(\alpha/D)^{1/4}}{\sqrt{2\pi\sinh(t\sqrt{4D\alpha})}} \times \exp\left(-\frac{\sqrt{\alpha/D}}{2\sinh(t\sqrt{4D\alpha})}\left[\left(x_0^2+y^2\right)\cosh(t\sqrt{4D\alpha}) - 2xx_0\right]\right). \tag{49}$$

We may now derive the statistics of resetting using the propagator, (49). Equation (45) together with Eq. (49) implies

$$P_{\text{no res}}(x,t|x_0,0) = \frac{(\alpha/D)^{1/4}}{\sqrt{2\pi\sinh(t\sqrt{4D\alpha})}} \times \exp\left(-\frac{\sqrt{\alpha/D}}{2\sinh(t\sqrt{4D\alpha})}\left[\left(x_0^2+x^2\right)\cosh(t\sqrt{4D\alpha}) - 2x_0x\right]\right). \tag{50}$$

Integrating Eq. (50) over x, we get the distribution of the first-reset time as

$$P_{\rm res}(t|x_0) = \int_{-\infty}^{\infty} {\rm d}y r(y) P_{\rm no\ res}(y,t|x_0,0) = \frac{\alpha(\alpha/D)^{1/4}}{\sqrt{\sinh(t\sqrt{4D\alpha})}} \exp\left(-x_0^2 \frac{\sqrt{\alpha/D}}{2} \tanh(t\sqrt{4D\alpha})\right) \times \frac{\sqrt{\alpha/D}\coth(t\sqrt{4D\alpha}) + x_0^2(\alpha/D)\mathrm{cosech}^2(t\sqrt{4D\alpha})}{(\alpha/D)^{5/4}\coth^{5/2}(t\sqrt{4D\alpha})}. \quad (51)$$

For the case $x_0 = 0$, Eqs. (50) and (51) reduce to simpler expressions:

$$P_{\rm no\ res}(x,t|x_0 = 0,0) = \frac{(\alpha/D)^{1/4}}{\sqrt{2\pi\ \sinh(t\sqrt{4D\alpha})}} \exp\left(-\frac{x^2\sqrt{\alpha/D}\coth(t\sqrt{4D\alpha})}{2}\right) \quad (52)$$

and

$$P_{\rm res}(t|x_0 = 0) = \sqrt{D\alpha}\frac{(\tanh(t\sqrt{4D\alpha}))^{3/2}}{\sqrt{\sinh(t\sqrt{4D\alpha})}}. \quad (53)$$

Equation (53) may be put in the scaling form

$$P_{\rm res}(t|x_0 = 0) = \sqrt{D\alpha}\,\mathcal{G}(t\sqrt{4D\alpha}), \quad (54)$$

with $\mathcal{G}(y) = \tanh(y)^{3/2}/\sqrt{\sinh(y)}$. Equation (53) yields the mean first-reset time $\langle t\rangle_{\rm res}$ for $x_0 = 0$, given by

$$\langle t\rangle_{\rm res} = \frac{(\Gamma(1/4))^2}{4\sqrt{2\pi D\alpha}}, \quad (55)$$

where Γ is the gamma function. Equations (53) and (55) yield the stationary spatial distribution upon using Eq. (30),

$$P_{\rm st}(x|x_0 = 0) = \frac{4\sqrt{D\alpha}(\alpha/D)^{1/4}}{(\Gamma(1/4))^2} \times \int_0^{\infty} \frac{{\rm d}t}{\sqrt{\sinh(t\sqrt{4D\alpha})}} \times \exp\left(-\frac{x^2\sqrt{\alpha/D}\coth(t\sqrt{4D\alpha})}{2}\right) = \frac{2^{3/4}(\alpha/D)^{1/4}}{\sqrt{\pi}\Gamma(1/4)}\left(\frac{x^2\sqrt{\alpha/D}}{2}\right)^{1/4} K_{1/4}\left(\frac{x^2\sqrt{\alpha/D}}{2}\right), \quad (56)$$

where $K_n(x)$ is the nth-order modified Bessel function of the second kind. Equation (56) implies that the stationary distribution is symmetric around $x = 0$, which is expected since the resetting rate is symmetric around $x_0 = 0$. The stationary distribution, (56), may be put in the scaling form

$$P_{\rm st}(x|x_0 = 0) = \frac{2^{3/4}(\alpha/D)^{1/4}}{\sqrt{\pi}\Gamma(1/4)}\mathcal{R}\left(\frac{x}{(D/\alpha)^{1/4}}\right), \quad (57)$$

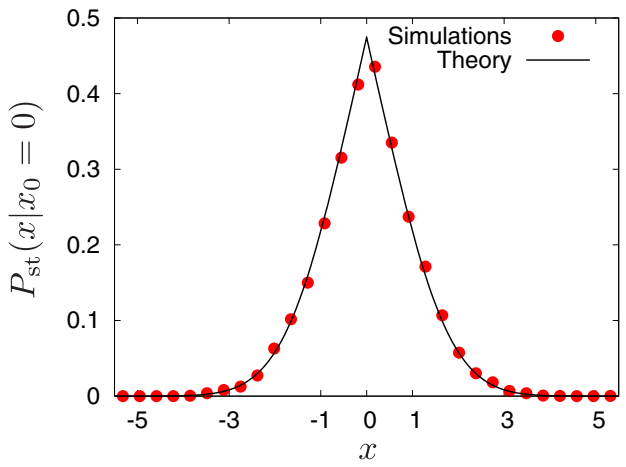

FIG. 2. Theory versus simulation results for the stationary spatial distribution of a free Brownian particle undergoing parabolic resetting. Circles denote simulation results, while the line represents the exact analytical expression given in Eq. (56). Numerical results were obtained from 10^4 independent simulations of the Langevin dynamics described in Sec. II A. Error bars associated with the data points are smaller than the symbol size. Parameter values are $D = 1.0, \alpha = 0.5$.

where the scaling function is given by $\mathcal{R}(y) = (y^2/2)^{1/4}K_{1/4}(y^2/2)$.

The result, (56), is checked in simulations in Fig. 2. The simulations involved numerically integrating the dynamics described in Sec. II A, with the integration time step equal to 0.01. Using $\int_0^{\infty} {\rm d}t t^{\mu-1}K_\nu(t) = 2^{\mu-2}\Gamma(\frac{\mu}{2} - \frac{\nu}{2})\Gamma(\frac{\mu}{2} + \frac{\nu}{2})$ for $|{\rm Re}\nu| < |{\rm Re}\mu|$ [49], we find that $P_{\rm st}(x|x_0 = 0)$, given by Eq. (56), is correctly normalized to unity. Moreover, using the results that as $x \to 0$, we have $K_\nu(x) = \frac{\Gamma(\nu)}{2}(\frac{x}{2})^{-\nu}$ for Re $\nu > 0$, and that as $x \to \infty$, we have $K_\nu(x) = (\frac{\pi}{2x})^{1/2}\exp(-x)$ for real x [49], we get

$$P_{\rm st}(x|x_0 = 0) \sim \begin{cases} \frac{(\alpha/D)^{1/4}}{\sqrt{\pi}} & \text{for} \quad x \to 0, \\ \exp(-x^2\sqrt{\alpha/D}/2) & \text{for} \quad |x| \to \infty. \end{cases} \quad (58)$$

Using Eq. (56) and the result ${\rm d}K_{1/4}(x)/{\rm d}x = -(1/2)(K_{3/4}(x) + K_{5/4}(x))$, it may be easily shown that as $x \to 0^{\pm}$, one has ${\rm d}P_{\rm st}(x|x_0 = 0))/{\rm d}x = \mp\sqrt{\alpha/D}\Gamma(3/4)/(\sqrt{\pi}\Gamma(1/4))$, thereby implying that the first derivative of $P_{\rm st}(x|x_0 = 0)$ is discontinuous at $x = 0$. We thus conclude that the spatial distribution $P_{\rm st}(x|x_0 = 0)$ exhibits a cusp singularity at $x = 0$. This feature of cusp singularity at the resetting location $x_0 = 0$ is also seen in the stationary distribution, (43), and is a signature of the steady state being a nonequilibrium one [16,21,32,33]. Note the existence of faster-than-exponential tails suggested by Eq. (58) in comparison to the exponential tails observed in the case of resetting at a constant rate, see Eq. (43). This is consistent with the fact that with respect to the case of resetting at a space-independent rate, a parabolic rate of resetting implies that the farther the particle is from $x_0 = 0$, the more enhanced is the probability that a resetting event takes place and, hence, the lower is the probability of finding the particle far away from the resetting location.

Let us consider the case of an overdamped Brownian particle that is trapped in a harmonic potential $V(x) = (1/2)\kappa x^2$, with $\kappa > 0$, and is undergoing Langevin dynamics, (1). At equilibrium, the distribution of the position of the particle is given by the Boltzmann-Gibbs distribution

$$P_{\rm eq}(x) = \exp(-\kappa x^2/2k_BT)/Z, \tag{59}$$

with $Z = \sqrt{2\pi k_BT/\kappa}$ being the partition function. Comparing Eqs. (58) and (59), we see that using a harmonic potential with a suitable κ, the stationary distribution of a free Brownian particle undergoing parabolic resetting may be made to match in the tails with the stationary distribution of a Brownian particle trapped in the harmonic potential and evolving in the absence of any resetting. On the other hand, the cusp singularity in the former cannot be achieved with Langevin dynamics in any harmonic potential without the inclusion of resetting events.

Let us note that the stationary states, (43) and (56), are entirely induced by the dynamics of resetting. Indeed, in the absence of any resetting, the dynamics of a free-diffusing particle does not allow for a long-time stationary state, since in the absence of a force, there is no way in which the motion of the particle can be bounded in space. On the other hand, in the presence of resetting, the dynamics of repeated relocation to a given position in space can effectively compete with the inherent tendency of the particle to spread out in space, leading to a bounded motion and, hence, a relaxation to a stationary spatial distribution at long times. In the next section, we consider the situation where the particle, even in the absence of any resetting, has a localized stationary spatial distribution and investigate the change in the nature of the spatial distribution of the particle owing to the inclusion of resetting events.

C. Particle trapped in a harmonic potential with energy-dependent resetting

We now introduce a resetting problem that is relevant in physics: an overdamped Brownian particle immersed in a thermal bath at temperature T and trapped with a harmonic potential centered at the origin, $V(x) = (1/2)\kappa x^2$, where $\kappa > 0$ is the stiffness constant of the harmonic potential. The particle, initially located at $x_0 = 0$, may be reset at any time t to the origin with a probability that depends on the energy of the particle at time t. The dynamics is shown schematically in Fig. 3. For purposes of illustration of the nontrivial effects of resetting, we consider the space-dependent reseting rate

$$r(x) = \frac{3}{2\tau_c}\frac{V(x)}{k_BT} = \frac{3}{4}\frac{\mu^2\kappa^2}{D}x^2, \tag{60}$$

where we use $D = k_BT\mu$ in obtaining the second equality. Note that the resetting rate is proportional to the energy of the particle (in units of k_BT) divided by the time scale $\tau_c \equiv 1/\mu\kappa$, which characterizes the relaxation of the particle in the harmonic potential in the absence of any resetting. In this way, it is ensured that the rate of resetting, (60), has units of inverse time. Note also that in the absence of any resetting, the particle relaxes to an equilibrium stationary state with a spatial

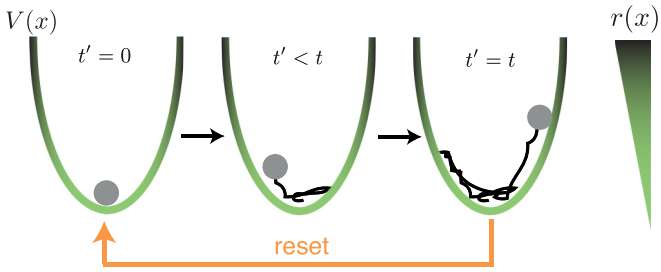

FIG. 3. Illustration of the energy-dependent resetting of a Brownian particle moving in a harmonic potential. A Brownian particle (gray circle) immersed in a thermal bath at temperature T moves with diffusion coefficient D, with its motion being confined by a harmonic potential $V(x) = \kappa x^2/2$ (green area), where κ is the stiffness constant. Here, x is the position of the particle with respect to the center of the potential. The particle, initially located in the trap center ($t' = 0$; left panel), diffuses at subsequent times in the energy landscape ($t' < t$; middle panel), until a resetting event occurs at time $t' = t$ (right panel). The black curve represents the history of the particle from $t' = 0$ up to the time corresponding to each snapshot. The rate of resetting (right color bar) is proportional to the instantaneous energy of the particle, and therefore, a reset is more likely to take place as the particle climbs up the potential.

distribution given by the usual Boltzmann-Gibbs form:

$$P_{\rm st}^{r(x)=0}(x) = \sqrt{\frac{\kappa}{2\pi k_BT}}\exp\left(-\frac{\kappa x^2}{2k_BT}\right). \tag{61}$$

Using $F(x) = -\partial_x V(x) = -\kappa x$ and expression (60) for the resetting rate in Eq. (19), we find that the potential of the corresponding quantum mechanical problem is given by

$$V_{\rm q}(x) = \frac{\mu^2(F(x))^2}{4D} + \frac{\mu F'(x)}{2} + r(x) = \frac{\mu^2\kappa^2x^2}{D} - \frac{\mu\kappa}{2}, \tag{62}$$

where we have used $F'(x) = -\kappa$. From Eqs. (15) and (16), we obtain

$$\begin{aligned} &P_{\rm no\ res}(x,t|x_0 = 0,0) \\ &= \exp\left(\frac{\mu}{2D}\int_{x_0}^{x} F(x){\rm d}x\right) \\ &\quad\times \exp\left(\frac{\mu\kappa t}{2}\right)\langle x|\exp(-H_{\rm q}t)|x_0 = 0\rangle \\ &= \exp\left(-\frac{x^2}{4D\tau_c}\right)\exp\left(\frac{t}{2\tau_c}\right)\langle x|\exp(-H_qt)|x_0 = 0\rangle, \end{aligned} \tag{63}$$

where the quantum Hamiltonian is given by

$$H_q = -\frac{1}{2m_q}\frac{\partial^2}{\partial x^2} + \frac{\mu^2\kappa^2x^2}{D}, \quad m_q = \frac{1}{2D}, \quad \hbar = 1. \tag{64}$$

We thus find that the propagator $\langle x|\exp(-H_qt)|x_0 = 0\rangle$ is given by the propagator of a quantum harmonic oscillator, which has been calculated in Sec. III B. In fact, the Hamiltonian given by Eq. (64) is identical to that given by Eq. (46) with the identification $\alpha = \mu^2\kappa^2/D = 1/D\tau_c^2$, so that by substituting

$x_0 = 0$ and $\alpha = 1/(D\tau_c^2)$ in Eq. (49), we obtain

$$\langle x|\exp(-H_q t)|x_0 = 0\rangle = \frac{1}{\sqrt{2\pi D\tau_c \sinh(2t/\tau_c)}} \exp\left(-\frac{x^2}{2D\tau_c}\coth(2t/\tau_c)\right). \tag{65}$$

From Eqs. (64) and (65), we obtain

$$P_{\text{no res}}(x,t|x_0 = 0,0) = \frac{\exp(t/2\tau_c)}{\sqrt{2\pi D\tau_c \sinh(2t/\tau_c)}} \exp\left(-\frac{x^2}{2D\tau_c}\left[\frac{1}{2}+\coth(2t/\tau_c)\right]\right). \tag{66}$$

Following Eq. (20), we may now calculate the probability of the first-reset time by using Eq. (66) to get

$$P_{\text{res}}(t|x_0 = 0) = \frac{\exp(t/2\tau_c)}{\sqrt{2\pi D\tau_c \sinh(2t/\tau_c)}} \times \int_{-\infty}^{\infty} dx \frac{3x^2}{4D\tau_c^2} \exp\left(-\frac{x^2}{2D\tau_c}\left[\frac{1}{2}+\coth(2t/\tau_c)\right]\right) = \frac{3\exp(t/2\tau_c)}{4\tau_c}\sqrt{\frac{1}{\sinh(2t/\tau_c)(1/2+\coth(2t/\tau_c))^3}}, \tag{67}$$

which may be checked to be normalized: $\int_0^\infty dt\, P_{\text{res}}(t|x_0 = 0) = 1$. The first-reset time distribution, (67), may be written in the scaling form

$$P_{\text{res}}(t|x_0 = 0) = \frac{3}{4\tau_c}\mathcal{G}\left(\frac{2t}{\tau_c}\right), \tag{68}$$

with the scaling function given by $\mathcal{G}(y) = \exp(y/4)\sinh(y)^{-1/2}(1/2+\coth(y))^{-3/2}$.

The mean first-reset time, given by $\langle t\rangle_{\text{res}} \equiv \int_0^\infty dt\, P_{\text{res}}(t|x_0 = 0)$, equals

$$\langle t\rangle_{\text{res}} = \frac{4\tau_c}{\sqrt{3}}\,{}_2F_1\left(\frac{1}{8},\frac{1}{2};\frac{9}{8};-\frac{1}{3}\right), \tag{69}$$

where ${}_pF_q(a_1,a_2,\ldots,a_p;b_1,b_2,\ldots,b_q;x)$ is the generalized hypergeometric function. Introducing the variable $z \equiv 2t/\tau_c$ and using Eq. (67), we get

$$P_{\text{st}}(x|x_0 = 0) = \frac{1}{\langle t\rangle_{\text{res}}}\sqrt{\frac{\tau_c}{8\pi D}}\exp\left(-\frac{x^2}{4D\tau_c}\right) \times \int_0^\infty dz \frac{\exp(z/4)}{\sqrt{\sinh(z)}}\exp\left(-\frac{x^2\coth z}{2D\tau_c}\right) = \frac{1}{\langle t\rangle_{\text{res}}}\sqrt{\frac{\tau_c}{8\pi D}}\exp\left(-\frac{x^2}{4D\tau_c}\right) \times \frac{1}{2}\left(\frac{x^2}{4D\tau_c}\right)^{-1/4}\Gamma(1/8)\,W_{1/8,1/4}\left(\frac{x^2}{D\tau_c}\right), \tag{70}$$

where $W_{\mu,\nu}$ is Whittaker's W function.

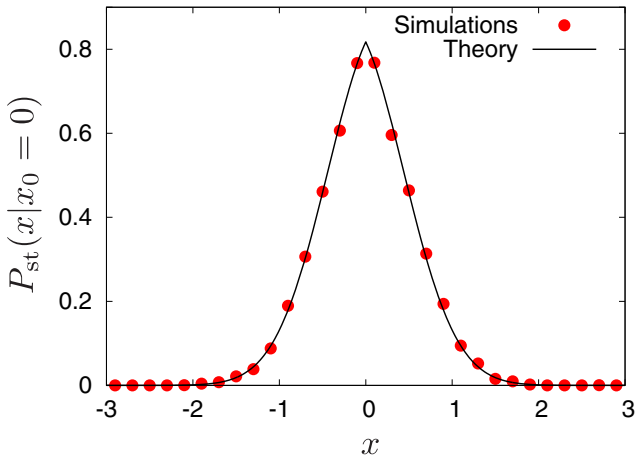

FIG. 4. Theory versus simulation results for the stationary spatial distribution of a Brownian particle trapped in a harmonic potential and undergoing energy-dependent resetting. Circles denote simulation results, while the line represents the exact analytical expression given in Eq. (72). Numerical results were obtained from 10^4 independent simulations of the Langevin dynamics described in Sec. II A. Error bars associated with the data points are smaller than the symbol size. Parameter values are $D = 1.0$, $\tau_c = 0.5$.

Using Eq. (69) in Eq. (70), we obtain

$$P_{\text{st}}(x|x_0 = 0) = \frac{(1/8)\Gamma(1/8)}{{}_2F_1\left(\frac{1}{8},\frac{1}{2};\frac{9}{8};-\frac{1}{3}\right)} \times \sqrt{\frac{3}{8\pi D\tau_c}}\exp\left(-\frac{x^2}{4D\tau_c}\right)\left(\frac{4D\tau_c}{x^2}\right)^{1/4} \times W_{1/8,1/4}\left(\frac{x^2}{D\tau_c}\right), \tag{71}$$

which may be checked to be normalized to unity. We may write the stationary distribution in terms of a scaled position variable as

$$P_{\text{st}}(x|x_0 = 0) = \frac{(1/8)\Gamma(1/8)}{{}_2F_1\left(\frac{1}{8},\frac{1}{2};\frac{9}{8};-\frac{1}{3}\right)}\sqrt{\frac{3}{8\pi D\tau_c}}\mathcal{R}\left(\frac{x}{\sqrt{2D\tau_c}}\right), \tag{72}$$

with $\mathcal{R}(y) \equiv \exp(-y^2/2)(2/y^2)^{1/4}\,W_{1/8,1/4}(2y^2)$ being the scaling function. Expression (72) is checked in simulations in Fig. 4. The simulations involved numerically integrating the dynamics described in Sec. II A, with the integration time step equal to 0.01. Using the results that as $x \to 0$, we have $W_{k,\mu}(x) = \frac{\Gamma(2\mu)}{\Gamma(1/2+\mu-k)}x^{1/2-\mu}$ for $0 \leqslant \text{Re}\,\mu < 1/2$, $\mu \neq 0$, and that as $x \to \infty$, we have $W_{k,\mu}(x) \sim e^{-x/2}x^k$ for real x [49], we get

$$P_{\text{st}}(x|x_0 = 0) \sim \begin{cases} \frac{(1/8)\Gamma(1/8)}{{}_2F_1(1/8,1/2;9/8;-1/3)}\frac{\sqrt{3/8D\tau_c}}{\Gamma(5/8)} & \text{for } x \to 0, \\ \exp\left(-\frac{3x^2}{4D\tau_c}\right) & \text{for } |x| \to \infty. \end{cases}$$

We see again the existence of a cusp at the resetting location $x_0 = 0$, similarly to all other cases studied in this paper.

The results in this subsection could inspire future experimental studies using optical tweezers in which the resetting

protocol could be effectively implemented by using feedback control [3,5,6]. Interestingly, colloidal and molecular gel and glassy systems show hopping motion of their constituent particles between potential traps or "cages," the latter originating from the interaction of the particles with their neighbors [50]. This phenomenon is also exhibited by out-of-equilibrium glasses and gels during the process of aging [51]. Our results in this section could provide valuable insights into the aforementioned dynamics, since the emergent potential cages may be well approximated by harmonic traps and the hopping process as a resetting event.

IV. SHORTCUTS TO CONFINEMENT

A hallmark of the examples solved exactly in Sec. III using our path-integral formalism is the existence of stationary distributions with prominent *cusp singularities* (see Figs. 2 and 4). These examples demonstrate that the particle can be confined around a prescribed location by using appropriate space-dependent rates of resetting.

In physics and nanotechnology, the issue of achieving accurate control of the fluctuations of small particles is nowadays attracting considerable attention [52–54]. For instance, using optical tweezers and noisy electrostatic fields, it is now possible to control accurately the amplitude of fluctuations of the position of a Brownian particle [55,58,59]. Such fluctuations may be characterized by an effective temperature. Experiments have reported effective temperatures of a colloidal particle in water up to 3000 K [52] and have recently been used to design colloidal heat engines at the mesoscopic scale [55,60]. Effective confinement of small systems is of paramount importance for the success of quantum-based computations with, e.g., cold atoms [56,57].

Does stochastic resetting provide an efficient way to reduce the amplitude of fluctuations of a Brownian particle, thereby providing a technique to reduce the associated effective temperature? We now provide some insights into this question.

Consider the following example of a nonequilibrium protocol: (i) a Brownian particle is initially confined in a harmonic trap with a potential $V(x) = (1/2)\kappa x^2$ for a sufficiently long time that it is in an equilibrium state with spatial distribution $P_{\rm eq}(x) = \exp(-\kappa x^2/2k_BT)/Z$, where $Z = \sqrt{2\pi k_BT/\kappa}$; (ii) the space-dependent (parabolic) resetting rate $r(x) = (3/2\tau_c)V(x)/k_BT$, with $\tau_c = (1/\mu\kappa)$, is suddenly switched on by an external agent—in other words, the rate of resetting is instantaneously quenched from $r(x) = 0$ to $r(x) = (3/4)(\mu^2\kappa^2/D)x^2$; and (iii) the particle is allowed to relax to a new stationary state in the presence of the trapping potential and parabolic resetting. At the end of the protocol, the particle relaxes to the stationary distribution $P_{\rm st}(x)$ given by Eq. (71).

We first note that before the sudden switching-on of the resetting dynamics, which we assume to happen at reference time $t = 0$, the mean-squared displacement of the particle is given by

$$\langle x^2(0)\rangle = \frac{k_BT}{\kappa}, \tag{73}$$

which follows from the equilibrium distribution before the resetting is switched on and is in agreement with the equipartition theorem $\kappa\langle x^2(0)\rangle/2 = k_BT/2$. After the sudden switching-on of the space-dependent rate of resetting, the variance of the position of the particle relaxes at long times to the stationary value

$$\langle x^2(\infty)\rangle = \frac{k_BT/\kappa}{\sqrt{3}\,{}_2F_1\left(\frac{1}{8},\frac{1}{2};\frac{9}{8};-\frac{1}{3}\right)} \simeq 0.59\frac{k_BT}{\kappa}, \tag{74}$$

as follows from Eq. (71). The resetting dynamics induces in this case a reduction by about 40% of the variance of the position of the particle with respect to its initial value. We note that such a reduction of the amplitude of fluctuations of the particle could also have been achieved by performing a sudden quench of the stiffness of the harmonic potential by increasing its value from κ to $\kappa' \simeq (1/0.59)\kappa \simeq 1.7\kappa$, without the need for switching-on of resetting events. To understand the difference between the two scenarios, it is instructive to compare the time evolution of the mean-squared displacement $\langle x^2(t)\rangle$ towards the stationary value in the two cases (see inset in Fig. 5). We observe that resetting leads to the same degree of confinement in a shorter time. For the case in which the stiffness of the potential is quenched from

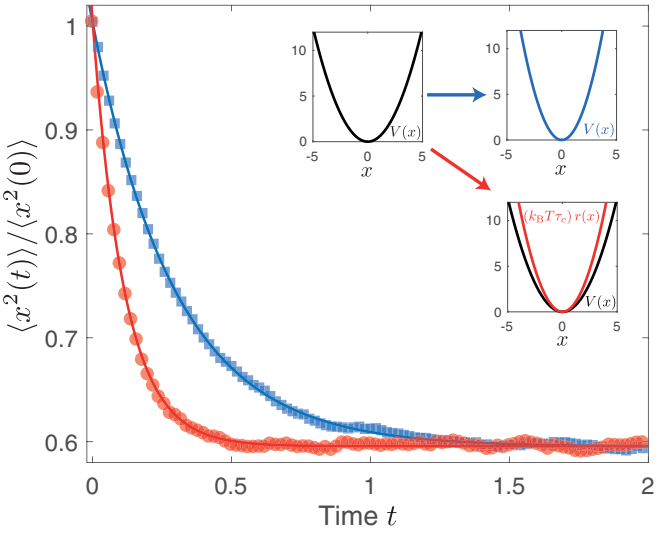

FIG. 5. Shortcut to particle confinement. Confinement of a Brownian particle using harmonic potentials and space-dependent rates of resetting. Symbols represent simulation results for relaxation processes of 10^5 noninteracting Brownian particles that are initially in equilibrium in a harmonic potential $V(x) = (1/2)\kappa x^2$. Blue circles represent the mean-squared displacement of the particle, in units of $\langle x^2(0)\rangle$, after an instantaneous quench to a harmonic potential with stiffness $\kappa' = 1.7\kappa$ (blue arrow in the inset). Red circles, on the other hand, represent the mean-squared displacement of the particle, in units of $\langle x^2(0)\rangle$, after an instantaneous quench of the rate of resetting from $r(x) = 0$ to $r(x) = (3/4)(\mu^2\kappa^2/D)x^2$ (red arrow in the inset). For the case in which the stiffness of the potential is quenched from κ to κ', it is easily seen that $\langle x^2(t)\rangle = \langle x^2(0)\rangle\exp(-2\mu k't) + (D/(\mu k'))[1 - \exp(-2\mu k't)]$, thereby implying a relaxation time scale $\tau_{\rm quench} = 1/(2\mu k')$ and yielding the blue curve in the figure. Note that the time on the x axis is measured in units of $\tau_c = 1/\mu\kappa$. The red curve, depicting the process of relaxation in the presence of resetting, may be fitted to a good approximation to $A + Be^{-t/\tau_{\rm reset}}$. One observes that $\tau_{\rm reset} \approx \tau_{\rm quench}/3$. Parameter values are $D = 1$, $\kappa = 1$, and $\mu = 10$.

κ to κ', it is easily seen that $\langle x^2(t)\rangle = \langle x^2(0)\rangle \exp(-2\mu k' t) + (D/(\mu k'))[1 - \exp(-2\mu k' t)]$, thereby implying a relaxation time scale $\tau_{\rm quench} = 1/(2\mu k')$ and yielding the corresponding curve in Fig. 5. The other curve depicting the process of relaxation in the presence of resetting may be fitted to a good approximation to $A + Be^{-t/\tau_{\rm reset}}$. One observes that $\tau_{\rm reset} \approx \tau_{\rm quench}/3$. Thus, for the example at hand, we may conclude that a sudden quench of resetting profiles provides a shortcut to confinement of the position of the particle to a desired degree with respect to a potential quench. Similar conclusions were arrived at for mean first-passage times of resetting processes and equivalent equilibrium dynamics [61].

It may be noted that the confinement protocol by a sudden quench of resetting profiles introduced above is amenable to experimental realization. Using microscopic particles trapped with optical tweezers [55,59] or feedback traps [58,62,63], it is now possible to measure and control the position of a Brownian particle with subnanometric precision. Recent experimental setups allow us to exert random forces on trapped particles, with a user-defined statistics for the random force [52,53,55,64]. The shortcut protocol using resetting could be explored in the laboratory by designing a feedback-controlled experiment with optical tweezers and by employing random-force generators according to, e.g., the protocol sketched in Fig. 3.

V. CONCLUSIONS AND OUTLOOK

In this paper, we have addressed the fundamental question of what happens when a continuously evolving stochastic process is repeatedly interrupted at random times by a sudden reset of the state of the process to a given fixed state. To this end, we studied the dynamics of an overdamped Brownian particle diffusing in force fields and resetting to a given spatial location at a rate that has an essential dependence on space, namely, the probability with which the particle resets is a function of the current location of the particle.

To address stochastic resetting in the aforementioned scenario, we employed a path-integral approach, discussed in detail in Eqs. (15)–(19) in Sec. II B 1. Invoking the Feynman-Kac formalism, we have obtained an equality that relates the probability of transition between different spatial locations of the particle before it encounters any reset to the quantum propagator of a suitable quantum mechanical problem (see Sec. II B 1). Using this formalism and elements from renewal theory, we have obtained closed-form analytical expressions for a number of statistics of the dynamics, e.g., the probability distribution of the first-reset time (Sec. II B 2), the time-dependent spatial distribution (Sec. II B 3), and the stationary spatial distribution (Sec. II B 4).

We have applied the method to a number of representative examples, including, in particular, those involving nontrivial spatial dependence of the rate of resetting. Remarkably, we have obtained the exact distributions of the aforementioned dynamical quantifiers for two nontrivial problems: the resetting of a free Brownian particle under "parabolic" resetting (Sec. III B) and the resetting of a Brownian particle moving in a harmonic potential at a resetting rate that depends on the energy of the particle (Sec. III C). For the latter case, we showed that using instantaneous quenching of resetting profiles allows us to restrict the mean-squared displacement of a Brownian particle to a desired value on a faster time scale than using instantaneous potential quenches. We expect that such a *shortcut to confinement* would provide novel insights in ongoing research on, e.g., engineered-swift-equilibration protocols [65,66] and shortcuts to adiabaticity [67–69].

Our work may also be extended to the treatment of systems of interacting particles, with the advantage that the corresponding quantum mechanical system can be treated effectively using tools of quantum physics and many-body quantum theory. Our approach also provides a viable method to calculate the path probabilities of complex stochastic processes. Such calculations are of particular interest in many contexts, e.g., in stochastic thermodynamics [70–73] and in the study of several biological systems such as molecular motors [14,74], active gels [75], and genetic switches [76,77]. As a specific application in this direction, our approach allows us to explore the physics of Brownian tunneling [78], an interesting stochastic resetting version of the well-known phenomenon of quantum tunneling, which serves to unveil the subtle effects resulting from stochastic resetting in, e.g., transport through nanopores [79].

ACKNOWLEDGMENT

E.R. thanks Ana Lisica and Stephan Grill for initial discussions, Ken Sekimoto and Luca Peliti for discussions on path integrals, and Domingo Sánchez and Juan M. Torres for discussions on quantum mechanics.

[1] R. Landauer, Irreversibility and heat generation in the computing process, IBM J. Res. Dev. **5**, 183 (1961).
[2] C. H. Bennett, Logical reversibility of computation, IBM J. Res. Dev. **17**, 525 (1973).
[3] A. Bérut, A. Arakelyan, A. Petrosyan, S. Ciliberto, R. Dillenschneider, and E. Lutz, Experimental verification of Landauer's principle linking information and thermodynamics, Nature **483**, 187 (2012).
[4] D. Mandal and C. Jarzynski, Work and information processing in a solvable model of Maxwell's demon, Proc. Natl. Acad. Sci. USA **109**, 11641 (2012).
[5] É. Roldán, I. A. Martínez, J. M. R. Parrondo, and D. Petrov, Universal features in the energetics of symmetry breaking, Nat. Phys. **10**, 457 (2014).
[6] J. V. Koski, V. F. Maisi, J. P. Pekola, and D. V. Averin, Experimental realization of a Szilard engine with a single electron, Proc. Natl. Acad. Sci. USA **111**, 13786 (2014).
[7] J. Fuchs, G. Goldt, and U. Seifert, Stochastic thermodynamics of resetting, Europhys. Lett. **113**, 60009 (2016).
[8] T. Mora, Physical Limit to Concentration Sensing Amid Spurious Ligands, Phys. Rev. Lett. **115**, 038102 (2015).

[9] É. Roldán, A. Lisica, D. Sánchez-Taltavull, and S. W. Grill, Stochastic resetting in backtrack recovery by RNA polymerases, Phys. Rev. E **93**, 062411 (2016).

[10] A. Lisica, C. Engel, M. Jahnel, É. Roldán, E. A. Galburt, P. Cramer, and S. W. Grill, Mechanisms of backtrack recovery by RNA polymerases I and II, Proc. Natl. Acad. Sci. USA **113**, 2946 (2016).

[11] D. T. Gillespie, E. Seitaridou, and C. A. Gillespie, The small-voxel tracking algorithm for simulating chemical reactions among diffusing molecules, J. Chem. Phys. **141**, 234115 (2014).

[12] P. Hanggi, P. Talkner, and M. Borkovec, Reaction-rate theory: Fifty years after Kramers, Rev. Mod. Phys. **62**, 251 (1990).

[13] I. Neri, É. Roldán, and F. Jülicher, Statistics of Infima and Stopping Times of Entropy Production and Applications to Active Molecular Processes, Phys. Rev. X **7**, 011019 (2017).

[14] F. Jülicher, A. Ajdari, and J. Prost, Modeling molecular motors, Rev. Mod. Phys. **69**, 1269 (1997).

[15] B. Zamft, L. Bintu, T. Ishibashi, and C. J. Bustamante, Nascent RNA structure modulates the transcriptional dynamics of RNA polymerases, Proc. Natl. Acad. Sci. USA **109**, 8948 (2012).

[16] M. R. Evans and S. N. Majumdar, Diffusion with Stochastic Resetting, Phys. Rev. Lett. **106**, 160601 (2011).

[17] M. R. Evans and S. N. Majumdar, Diffusion with optimal resetting, J. Phys. A: Math. Theor. **44**, 435001 (2011).

[18] M. R. Evans and S. N. Majumdar, Diffusion with resetting in arbitrary spatial dimension, J. Phys. A: Math. Theor. **47**, 285001 (2014).

[19] C. Christou and A. Schadschneider, Diffusion with resetting in bounded domains, J. Phys. A: Math. Theor. **48**, 285003 (2015).

[20] S. Eule and J. J. Metzger, Non-equilibrium steady states of stochastic processes with intermittent resetting, New J. Phys. **18**, 033006 (2016).

[21] A. Nagar and S. Gupta, Diffusion with stochastic resetting at power-law times, Phys. Rev. E **93**060102(R) (2016).

[22] D. Boyer and C. Solis-Salas, Random Walks with Preferential Relocations to Places Visited in the Past and Their Application to Biology, Phys. Rev. Lett. **112**, 240601 (2014).

[23] S. N. Majumdar, S. Sabhapandit, and G. Schehr, Random walk with random resetting to the maximum position, Phys. Rev. E **92**, 052126 (2015).

[24] M. Montero and J. Villarroel, Monotonic continuous-time random walks with drift and stochastic reset events, Phys. Rev. E **87**, 012116 (2013).

[25] V. Méndez and D. Campos, Characterization of stationary states in random walks with stochastic resetting, Phys. Rev. E **93**, 022106 (2016).

[26] L. Kuśmierz, S. N. Majumdar, S. Sabhapandit, and G. Schehr, First Order Transition for the Optimal Search Time of Lévy Flights with Resetting, Phys. Rev. Lett. **113**, 220602 (2014).

[27] D. Campos and V Méndez, Phase transitions in optimal search times: How random walkers should combine resetting and flight scales, Phys. Rev. E **92**, 062115 (2015).

[28] A. Pal, A. Kundu, and M. R. Evans, Diffusion under time-dependent resetting, J. Phys. A: Math. Theor. **49**, 225001 (2016).

[29] D. Boyer, M. R. Evans, and S. N. Majumdar, Long time scaling behaviour for diffusion with resetting and memory, J. Stat. Mech. (2017) 023208.

[30] R. J. Harris and H. Touchette, Phase transitions in large deviations of reset processes, J. Phys. A: Math. Theor. **50**, 10LT01 (2017).

[31] X. Durang, M. Henkel, and H. Park, The statistical mechanics of the coagulation-diffusion process with a stochastic reset, J. Phys. A: Math. Theor. **47**, 045002 (2014).

[32] S. Gupta, S. N. Majumdar, and G. Schehr, Fluctuating Interfaces Subject to Stochastic Resetting, Phys. Rev. Lett. **112**, 220601 (2014).

[33] S. Gupta and A. Nagar, Resetting of fluctuating interfaces at power-law times, J. Phys. A: Math. Theor. **49**, 445001 (2016).

[34] R. Falcao and M. R. Evans, Interacting Brownian motion with resetting, J. Stat. Mech. (2017) 023204.

[35] L. Kuśmierz and E. Gudowska-Nowak, Optimal first-arrival times in Lévy flights with resetting, Phys. Rev. E **92**, 052127 (2015).

[36] S. Reuveni, Optimal Stochastic Restart Renders Fluctuations in First Passage Times Universal, Phys. Rev. Lett. **116**, 170601 (2016).

[37] U. Bhat, C. De Bacco, and S. Redner, Stochastic search with Poisson and deterministic resetting, J. Stat. Mech. (2016) 083401.

[38] A. Pal and S. Reuveni, First Passage Under Restart, Phys. Rev. Lett. **118**, 030603 (2017).

[39] A. Pal, Diffusion in a potential landscape with stochastic resetting, Phys. Rev. E **91**, 012113 (2015).

[40] D. Cox, *Renewal Theory* (Methuen, London, 1962).

[41] R. P. Feynman and A. R. Hibbs, *Quantum Mechanics and Path Integrals* (McGraw–Hill, New York, 2010).

[42] L. S. Schulman, *Techniques and Applications of Path Integration* (John Wiley and Sons, Chichester, UK, 1981).

[43] M. Kac, On distribution of certain Wiener functionals, Trans. Am. Math. Soc. **65**, 1 (1949).

[44] M. Kac, On some connections between probability theory and differential and integral equations, in *Proc. Second Berkeley Symp. Math. Stat. Prob.* (University of California Press, Berkeley, 1951).

[45] S. N. Majumdar, Brownian functionals in physics and computer science, Curr. Sci. **89**, 2076 (2005).

[46] In quantum mechanics, this time transformation is often called Wick's rotation in honor of Gian-Carlo Wick.

[47] K. Sekimoto, Langevin equation and thermodynamics, Prog. Theor. Phys. Suppl. **130**, 17 (1998).

[48] K. Sekimoto, *Stochastic Energetics* (Springer, Berlin, 2000).

[49] F. W. J. Olver, A. B. O. Daalhuis, D. W. Lozier, B. I. Schneider, R. F. Boisvert, C. W. Clark, B. R. Miller, and B. V. Saunders (eds.), *NIST Digital Library of Mathematical Functions*, Release 1.0.14 (NIST, Gaithersburg, MD, 2016); http://dlmf.nist.gov/.

[50] S. Roldán-Vargas, L. Rovigatti, and F. Sciortino, Connectivity, dynamics, and structure in a tetrahedral network liquid, Soft Matter **13**, 514 (2017).

[51] L. Berthier and G. Biroli, Theoretical perspective on the glass transition and amorphous materials, Rev. Mod. Phys. **83**, 587 (2011).

[52] I. A. Martínez, É. Roldán, J. M. R. Parrondo, and D. Petrov, Effective heating to several thousand kelvins of an optically trapped sphere in a liquid, Phys. Rev. E **87**, 032159 (2013).

[53] A. Bérut, A. Petrosyan, and S. Ciliberto, Energy flow between two hydrodynamically coupled particles kept at different effective temperatures, Europhys. Lett. **107**, 60004 (2015).

[54] E. Dieterich, J. Camunas-Soler, M. Ribezzi-Crivellari, U. Seifert, and F. Ritort, Single-molecule measurement of

the effective temperature in non-equilibrium steady states, Nat. Phys. **11**, 971 (2015).
[55] I. A. Martínez, É. Roldán, L. Dinis, and R. A. Rica, Colloidal heat engines: A review, Soft Matter **13**, 22 (2017).
[56] J. I. Cirac and P. Zoller, Quantum Computations with Cold Trapped Ions, Phys. Rev. Lett. **74**, 4091 (1995).
[57] I. Bloch, Ultracold quantum gases in optical lattices, Nat. Phys. **1**, 23 (2005).
[58] M. Gavrilov, R. Chétrite, and J. Bechhoefer, Direct measurement of nonequilibrium system entropy is consistent with Gibbs-Shannon form, arXiv:1703.07601.
[59] S. Ciliberto, Experiments in Stochastic Thermodynamics: Short History and Perspectives, Phys. Rev. X **7**, 021051 (2017).
[60] I. A. Martínez, É. Roldán, L. Dinis, D. Petrov, J. M. R. Parrondo, and R. A. Rica, Brownian Carnot engine, Nat. Phys. **12**, 67 (2016).
[61] M. R. Evans, S. N. Majumdar, and K. Mallick, Optimal diffusive search: Nonequilibrium resetting versus equilibrium dynamics, J. Phys. A **46**, 185001 (2013).
[62] M. Gavrilov, Y. Jun, and J. Bechhoefer, Real-time calibration of a feedback trap, Rev. Sci. Instrum. **85**, 095102 (2014).
[63] Y. Jun and J. Bechhoefer, Virtual potentials for feedback traps, Phys. Rev. E **86**, 061106 (2012).
[64] I. A. Martínez, É. Roldán, L. Dinis, D. Petrov, and R. A. Rica, Adiabatic Processes Realized with a Trapped Brownian Particle, Phys. Rev. Lett. **114**, 120601 (2015).
[65] I. A. Martínez, A. Petrosyan, D. Guéry-Odelin, E. Trizac, and S. Ciliberto, Engineered swift equilibration of a Brownian particle, Nat. Phys. **12**, 843 (2016).
[66] L. Granger, L. Dinis, J. M. Horowitz, and J. M. R. Parrondo, Reversible feedback confinement, Europhys. Lett. **115**, 50007 (2016).
[67] S. Deffner, C. Jarzynski, and A. del Campo, Classical and Quantum Shortcuts to Adiabaticity for Scale-Invariant Driving, Phys. Rev. X **4**, 021013 (2014).
[68] J. Deng, Q. H. Wang, Z. Liu, P. Hänggi, and J. Gong, Boosting work characteristics and overall heat-engine performance via shortcuts to adiabaticity: Quantum and classical systems, Phys. Rev. E **88**, 062122 (2013).
[69] Z. C. Tu, Stochastic heat engine with the consideration of inertial effects and shortcuts to adiabaticity, Phys. Rev. E **89**, 052148 (2014).
[70] C. Jarzynski, Equalities and inequalities: Irreversibility and the second law of thermodynamics at the nanoscale, Annu. Rev. Condens. Matter Phys. **2**, 329 (2011).
[71] U. Seifert, Stochastic thermodynamics, fluctuation theorems and molecular machines, Rep. Prog. Phys. **75**, 12 (2012).
[72] A. Celani, S. Bo, R. Eichhorn, and E. Aurell, Anomalous Thermodynamics at the Microscale, Phys. Rev. Lett. **109**, 260603 (2012).
[73] S. Bo and A. Celani, Multiple-scale stochastic processes: Decimation, averaging and beyond, Phys. Rep. **670**, 1 (2017).
[74] T. Guérin, J. Prost, and J.-F. Joanny, Motion Reversal of Molecular Motor Assemblies Due to Weak Noise, Phys. Rev. Lett. **106**, 068101 (2011).
[75] A. Basu, J.-F. Joanny, F. Jülicher, and J. Prost, Thermal and non-thermal fluctuations in active polar gels, Eur. Phys. J. E **27**, 149 (2008).
[76] R. Perez-Carrasco, P. Guerrero, J. Briscoe, and K. M. Page, Intrinsic noise profoundly alters the dynamics and steady state of morphogen-controlled bistable genetic switches, PLoS Comput. Biol. **12**, e1005154 (2016).
[77] D. Schultz, A. M. Walczak, J. N. Onuchic, and P. G. Wolynes, Extinction and resurrection in gene networks, Proc. Natl. Acad. Sci. USA **105**, 19165 (2008).
[78] E. Roldán and S. Gupta (unpublished).
[79] E. H. Trepagnier, A. Radenovic, D. Sivak, P. Geissler, and L. Liphardt, Controlling DNA capture and propagation through artificial nanopores, Nano Lett. **7**, 2824 (2007).